WARRANTS FOR GUARDRAILS ON EMBANKMENTS

Hayes E. Ross, Jr., and Edward R. Post, Texas Transportation Institute, Texas A&M University;
John F. Nixon and David Hustace, Texas Highway Department; and
Edward V. Kristaponis, Federal Highway Administration

The highway-vehicle-object simulation model, a computer model that describes an automobile and is capable of predicting the dynamic response of the automobile traversing selected terrain, was used to study the behavior of a standard-sized automobile traversing embankment side slopes at various speeds and departure angles. The accelerations obtained were used to compute a severity index that was then compared with a similarly computed severity index (from actual crash data) of a vehicle impacting a W-beam guardrail with posts on $6\frac{1}{4}$-ft spacing. An equal-severity curve was then developed that can be used as a guardrail installation criterion.

•WHEN a vehicle, traveling at a high speed, leaves the roadway and strikes a guardrail, a hazardous situation obviously exists. It is also hazardous when there is no guardrail and the vehicle must traverse the ditch. Neither event is desirable. Nevertheless, for a given type of guardrail, given ditch or embankment configuration, and given vehicle encroachment conditions, one situation will be less severe than the other.

To determine the need for guardrails on embankments, many highway engineers are using criteria developed by Glennon and Tamburri (11). Their study was based on a statistical analysis of accident information from the California state highways during 1963 and 1964. The two basic types of guardrail in use during the time of the accidents were a spring-mounted curved metal plate on 10-ft post spacing and a blocked-out W-section corrugated beam on 12-ft, 6-in. post spacing.

The primary type of guardrail used by the Texas Highway Department (THD) is a W-section corrugated beam on posts spaced on 6-ft, 3-in. centers, with no block-out of the rail from the post. Because the THD guardrail system differs considerably from the one in use during the California study (primarily in the post spacing), it was decided that criteria relevant to the THD system should be developed. The objective of this study was, therefore, to determine where it is safer to traverse an embankment than to impact the THD guardrail.

The approach of this study parallels that of Glennon and Tamburri (11) in that an equal-severity curve is established for determining the less severe alternative, guardrail or unprotected embankment. For an errant vehicle, the curve represents the combination of embankment heights and slopes that are equal in severity to impacting a particular guardrail. The major difference of the two approaches is the basis for measuring accident (guardrail impacts and embankment traversals) severity. Weighted severity values (11) were assigned to different occupant injury levels as determined from the accident reports. In the study described here, a combination of mathematical models and full-scale test data was used to determine vehicle accelerations during guardrail impacts and embankment traversals. Vehicle accelerations served as the measure of severity. In establishing need criteria, we believe that mathematical models and test data provide more flexibility than do accident records. Much of the subjectivity of accident records is removed. Although the criteria developed in this study pertain to a particular guardrail system, the methods used in the development are general, and any type of guardrail or embankment configuration can be investigated.

ESTABLISHING GUARDRAIL NEED

Approach

A mathematical model of an automobile (1), denoted herein as highway-vehicle-object simulation model (HVOSM), was used to determine the orientation and accelerations of a simulated automobile traversing various embankment configurations. A mathematical model (9) and full-scale test data (8, 10) were used to determine the accelerations of an automobile impacting a guardrail system similar to the THD system. Accelerations at the center of gravity of the automobile were used as the measure of severity. A severity index (SI), discussed in a report by Ross and Post (2), served to quantify the relative severity of each event for an unrestrained occupant.

To compare the severity of a vehicle impacting a guardrail with the severity of a vehicle traversing an embankment, one should use the same vehicle under the same encroachment conditions. These requirements were maintained as closely as possible. In the mathematical model studies of embankment encroachments, a 1963 Ford Galaxie was used. In most of the cases analyzed, a vehicle of similar size was used in the full-scale guardrail tests. Also, in most of the reported full-scale guardrail crash tests, the vehicle impacted at 60 mph and a 25-deg angle. Hence, for vehicle encroachment conditions, a 25-deg angle of departure and a speed of 60 mph were selected. These encroachment conditions are the criteria recommended for the structural design of guardrails (14).

A parameter study was made to evaluate the effects of encroachment conditions on the severity of an embankment traversal and a guardrail collision. The embankment in each case was a 3:1 side slope, 20 ft in height, with a flat-bottom ditch.

Embankment

The basic geometry of each embankment investigated consisted of a 10-ft shoulder adjoining a side slope of b:a and height H, with a flat-bottom ditch (Fig. 1). Slopes (b:a) of 2:1, 3:1, and 6:1 in combination with heights (H) of 10, 20, 30, and 50 ft were studied. In addition, a 3.25:1 slope with a height of 20 ft and a 4:1 slope with a height of 20 ft were studied. The reason for studying the latter two cases is explained later in the paper.

In the 14 embankment combinations studied, the simulated automobile was placed on the roadway with an initial velocity and encroachment angle θ_1. Throughout the maneuvers, the automobile was assumed to be out of control; that is, no attempt was made to steer the automobile.

In most cases (Table 1), the encroachment angle and speed of the automobile increased as the vehicle traversed the embankment slope. In all but the 6:1 slope combinations, the automobile became completely airborne (all tires off ground) for a period of time after leaving the shoulder. In traversing a 2:1 slope with a height of 10 ft, the automobile landed on the ditch bottom and then pitched over about its front end. For all other height and slope combinations, the automobile landed on the embankment slope after being airborne with no tendency to roll or pitch over.

Table 1 also gives the maximum average decelerations for a 50-msec period. These values were obtained by studying the computer output for those times when the larger decelerations occurred and then, by trial and error, selecting the 50-msec period with the highest average deceleration. The SI was computed from data given in another report (2).

Guardrail

The types of guardrail that can be studied by the Texas Transportation Institute's version of HVOSM are limited to those whose lateral resistance to vehicle penetration is independent of the longitudinal position of the vehicle contact point. Because the W-section guardrail on 6-ft, 3-in. post spacing does not fall in this category, the model could not be applied.

Two methods were used to investigate the severity of a guardrail collision. The first method was based on data from full-scale crash tests by Michie (8) and Beaton (10).

The second method was based on results obtained by mathematical equations presented by Olson (9).

A review of the literature revealed that no full-scale tests have ever been performed on the guardrail system now used in Texas for embankment protection. However, the tests conducted by Michie (8) and Beaton (10) were conducted on a guardrail system similar to the THD guardrail. The one difference between the two systems was that the "as-tested" rail was, in all but one case, blocked out from the post, whereas the THD rail butts against the post. The difference in the collision performance of the two systems is subject to conjecture. The possibility for snagging in the non-blocked-out system appears greater, and, if so, the severity of colliding with the THD system may be higher. If snagging does not occur, it seems reasonable to assume that the severity of impact would be similar for the two systems. This assumption is based on the fact that the lateral resistance of the two systems is essentially the same. In any case, it was hypothesized that the severity of impacting the THD system would be equal to or greater than that of the as-tested systems. As such, the criteria may be conservative as to the need for the THD guardrail system; i.e., more guardrail protection may be required by these criteria than is needed. On the other hand, the criteria are directly applicable to the as-tested system (8, 10).

The SI's of guardrail collisions conducted by Michie (8) were computed and are given in Table 2. These tests were selected on the basis of being conducted at an impact speed and angle of approximately 60 mph and 25 deg. Also, the vehicles used in these tests were similar in size and weight to the one used in the simulation studies. The SI was computed for longitudinal and lateral decelerations occurring over two time intervals; 50 msec and 325 to 450 msec. The longer time interval was measured from the instant of impact to the time when the automobile becomes parallel to the centerline of the guardrail. The SI was computed over the longer interval so that it could be compared with the work of Olson (9), which is presented later. As discussed in the report by Ross and Post (2), the tolerable deceleration limits for the two time intervals were based on an interpretation of the findings of Hyde (4).

An analysis of three full-scale crash tests conducted by Beaton (10) at impact conditions of approximately 60 mph and 25 deg is given in Table 3. Because no acceleration-time data were reported by Beaton, the automobile decelerations perpendicular (G^{*}_{lat}) and parallel (G^{*}_{long}) to the guardrail were computed from the following equations developed by Olson (9):

$$G^{*}_{lat} = \frac{V_I^2 \sin^2(\theta)}{2g\{AL \sin(\theta) - B[1 - \cos(\theta)] + D\}} \tag{1}$$

$$G^{*}_{long} = \mu\, G^{*}_{lat} \tag{2}$$

where

V_I = impact velocity,
θ = impact angle,
AL = distance from front bumper to center of gravity,
$2B$ = width of vehicle (B = one-half of vehicle width),
D = lateral dynamic displacement of barrier, and
μ = coefficient of friction between vehicle and barrier [a value of 0.3 was used (Table A1, 9)].

The primary assumption in developing these equations was that the deceleration was constant from impact to the time in which the automobile becomes parallel to the guardrail. Olson (9) demonstrated that these equations were accurate within ±20 percent.

To compute an SI we must transform the decelerations computed by Eqs. 1 and 2 to the decelerations along the automobile coordinate system axes. This was accomplished with the following two transformation equations:

$$G_{lat} = G^{*}_{lat}\,[\cos(\theta) - \mu \sin(\theta)] \tag{3}$$

Figure 1. Embankment geometry and center-of-gravity path of automobile.

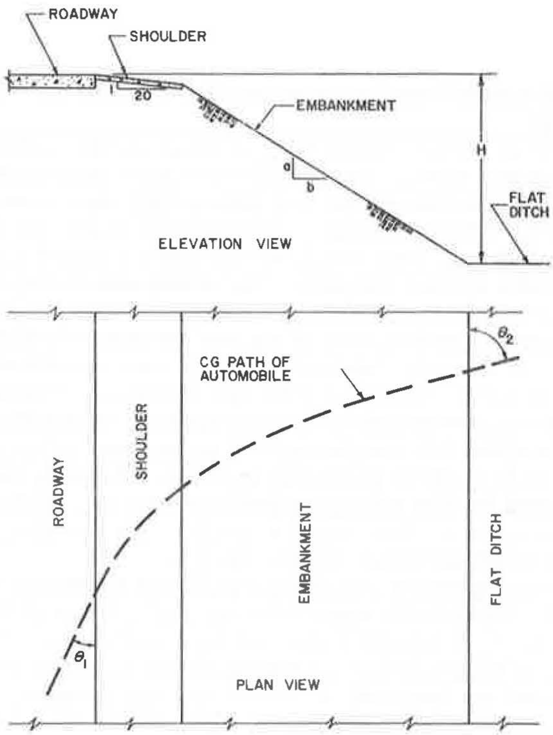

Table 1. Simulation results on embankments of various heights and slopes.

	Terrain		Automobile							
Run No.	Embankment Height (ft)	Embankment Slope (b:a)	Maximum Roll Angle (deg)	Maximum Pitch Angle (deg)	Angle Automobile Contacts Flat Ditch (deg)	Speed Automobile Contacts Flat Ditch (deg)	Average Deceleration >50 msec G_{long}	G_{lat}	G_{vert}	SI
1	10	2:1	33	RO[a]	24	60	2.6	3.4	4.7	1.1[b]
2	10	3:1	29	10	25	61	0.2	0.6	5.3	0.9
3	10	6:1	11	5	29	62	0.1	0.3	2.2	0.4
4	20	2:1	48	15	24	62	2.6	4.9	6.3	1.5
5	20	3:1	30	12	40	62	1.3	0.8	7.6	1.3
6	20	6:1	11	5	34	65	0.1	0.4	2.8	0.5
7	20	3.25:1	27	10	37	64	1.3	0.7	4.5	0.8
8	20	4:1	20	9	30	64	—	0.5	3.7	0.6
9	30	2:1	47	23	32	58	0.3	1.3	6.8	1.2
10	30	3:1	29	13	36	66	0.4	0.9	4.9	0.8
11	30	6:1	11	5	33	67	0.0	0.6	3.5	0.6
12	50	2:1	47	26	66	55	7.6	3.4	9.7	2.1
13	50	3:1	29	13	43	68	1.2	1.3	6.4	1.1
14	50	6:1	11	6	43	70	0.2	0.5	3.7	0.6

Note: Encroachment speed = 60 mph, shoulder width = 10 ft, encroachment angle (θ_1) = 25 deg, and shoulder slope = 20:1.

[a]Automobile rolled over about its front end as it contacted flat ditch after being airborne.

[b]Severity index when contact with flat ditch occurs (just prior to roll-over).

Table 2. Guardrail full-scale crash tests (8).

	Guardrail				Automobile								
								Decelerations (G)					
								50 msec			325 to 450 msec		
Test No.	Post	Blockout	Post Embedment (in.)	Dynamic Displacement (ft)	Weight (lb)	Impact Speed (mph)	Impact Angle (deg)	G_{long}	G_{lat}	SI[a]	G_{long}	G_{lat}	SI[b]
101	8- by 8-in. wood	8-in. wood	36	4.25	4,042	55	31	4.6	4.5	1.1	2.9	3.1	0.9
103	8- by 8-in. wood	8-in. wood	36	2.84	4,123	60	22	3.1	6.1	1.3	2.2	3.3	0.9
119	6B8.5	None	42	2.74	4,169	53	30	4.5	4.4	1.1	2.3	2.7	0.8
120	6B8.5	1-6B8.5	42	4.05	3,813	57	28	3.9	6.6	1.4	2.9	3.5	1.0
121	6B8.5	2-6B8.5	42	3.10	4,478	56	27	3.6	6.7	1.5	1.9	3.3	0.9
122	6B8.5	2-6B8.5	42	4.95	4,570	63	25	3.9	7.6	1.6	2.3	3.9	1.0

Note: Rail height = 27 in. and post spacing = 6 ft, 3 in. All rail members tested were steel W-beam.

[a]G_{XL} = 7 and G_{YL} = 5 (Appendix B, 2). [b]G_{XL} = 6 and G_{YL} = 4 (Appendix B, 2).

$$G_{long} = G^{*}_{lat} [\sin(\theta) - \mu \cos(\theta)] \tag{4}$$

Observations of high-speed photography show that, for the time interval between impact and maximum guardrail displacement (dynamic displacement), the heading angle of the automobile changes only slightly. It is during this interval that the maximum deceleration usually occurs. Therefore, in applying the preceding transformation equations, the initial impact angle was used.

A comparison of the SI's computed for the California tests in Table 3 with those in Table 2 further demonstrates that the mathematical equations presented by Olson (9) provide reasonable results. Equations 1 through 4 were used to predict the severity of guardrail collisions for various impact speeds and angles, as described later in this paper.

Comparison of Relative Severities

The SI's of embankment traversals (Table 1) are shown in Figure 2. Superimposed on the figure is the range of SI's for impacts with the guardrail from Tables 2 and 3. The range of SI's shown in Figure 2 for the guardrail was based on accelerations averaged over the longer time duration.

It was anticipated that the SI would increase as the embankment height increased for a given slope. However, this was not always the case, as shown in Figure 2. Two good examples of this anomaly were the SI's for a 2:1 slope with a 20-ft fill height and for a 3:1 slope with a 20-ft fill height (runs 4 and 5, Table 1). Both values were considerably higher than anticipated. Examination of the output from runs 4 and 5 showed that, when the vehicle reached the flat-bottom ditch, both the front and rear bumpers of the automobile simultaneously contacted and penetrated the terrain, causing large resistive forces. In other runs, front and rear bumper contact did not occur simultaneously; hence, the effect of bumper contact on the SI was not as pronounced.

Additional runs (runs 7 and 8, Table 1) were made on a 20-ft fill height to determine the variation of the SI between a 3:1 and 6:1 slope because of the large difference in the index between these slopes. As seen in Figure 2, flattening the slope from a 3:1 to a 3.25:1 and to a 4:1 resulted in a considerable reduction in the SI. A sharp transition was therefore found to exist in the SI at a slope of about 3:1 for the 20-ft embankment height. As discussed, both front and rear bumper contact occurred simultaneously for the 2:1 and 3:1 slopes on a 20-ft fill height, and, as a consequence, the forces and accelerations were greatly increased. Front and rear bumper contact did not occur simultaneously for the 3.25:1 and 4:1 slopes. Vehicle attitude during initial contact with the ditch is therefore a significant factor influencing the relative severity of an embankment traversal.

Table 4 gives those combinations of embankment slope (measured as a ratio and in degrees) and height that are equal in severity to the upper bound, average, and lower bound guardrail severities. Each combination represents the intersection point of a given embankment height curve with a given guardrail severity line shown in Figure 2. For example, traversal of an embankment with a 3.14:1 (or 18-deg) slope, 20 ft in height, is equal in severity to an automobile impacting the guardrail, based on the average guardrail severity.

Equal-severity curves based on the upper and lower bound of guardrail severities are shown in Figure 3. The coordinates of the four points from which each curve was drawn were taken from Table 4. As shown in Figure 3, a line through a slope equal to 3:1 (dotted line) appears to be an average equal-severity curve. By the average curve, an embankment with a slope steeper than 3:1 should be protected, and, conversely, slopes flatter than 3:1 would not need guardrail protection.

Embankment heights of less than 10 ft were not investigated. Nevertheless, it seems reasonable to assume that a line through a 3:1 slope can also be used as the equal-severity curve for heights of 10 ft or less. Implementation of the criteria would be simplified in so doing.

For comparison with this study, other equal-severity curves are shown in Figure 4. The relation established by Glennon and Tamburri (11) was based on a statistical anal-

Table 3. Guardrail full-scale crash tests (10).

Test No.	Guardrail: Wood Post Blockout (in.)	Post Spacing (in.)	Post Embedment (in.)	Rail Height (in.)	Dynamic Displacement[a] (ft)	Automobile: Weight (lb)	Impact Speed (mph)	Impact Angle (deg)	Average Decelerations of 275 to 300 msec: G^*_{lat} (Eq. 1)	G^*_{long} (Eq. 2)	G_{lat} (Eq. 3)	G_{long} (Eq. 4)	SI
106	8	6-3	41	30	2.45	4,570	60	25	3.9	1.2	3.1	2.7	0.9
107	8	6-3	35	27	2.10	4,570	60	25	4.2	1.3	3.3	2.9	1.0
108	8	6-3	35	24	2.10	4,570	59	25	4.1	1.2	3.2	2.8	0.9

Note: AL = 7.95 ft and 2B = 6.5 ft. All rail members tested were steel W-beam, and posts (with 6[8.2 rubbing rail) were 8- by 8-in. wood.
[a]Dynamic displacement taken as 1.4 times permanent set (8).

Figure 2. Severity comparison of automobile traversing embankment and colliding with guardrail.

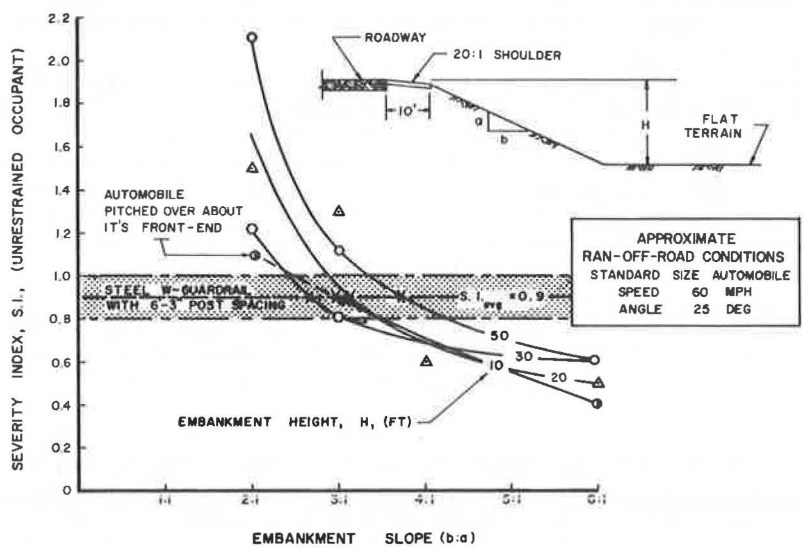

Table 4. Equal severity combinations.

Embankment Height (ft)	Upper Bound b:a	Upper Bound Deg	Average b:a	Average Deg	Lower Bound b:a	Lower Bound Deg
	Embankment Slope at Intersection of Guardrail and Embankment SI Curves[a]					
10	2.42:1	22	2.92:1	19	3.50:1	16
20	2.88:1	19	3.14:1	18	3.44:1	16
30	2.42:1	22	2.65:1	21	3.02:1	18
50	3.34:1	17	3.75:1	15	4.26:1	13

Note: For upper bound SI = 1.0, for average SI = 0.9, and for lower bound SI = 0.8.
[a]Values obtained from Figure 2.

Figure 3. Warrant for guardrails on embankments.

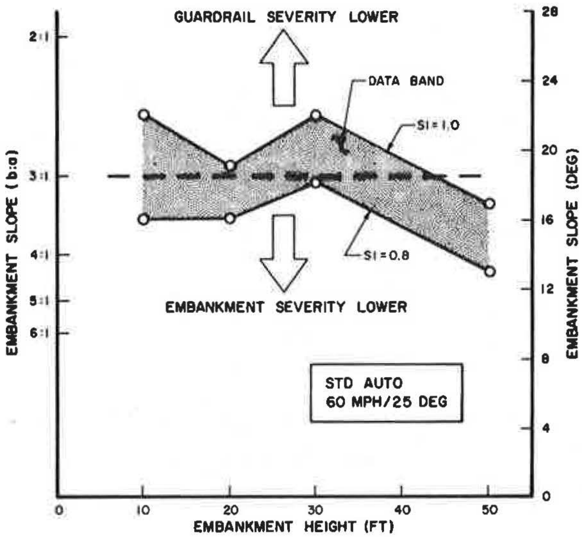

Figure 4. Comparison of warrants for guardrails on embankments.

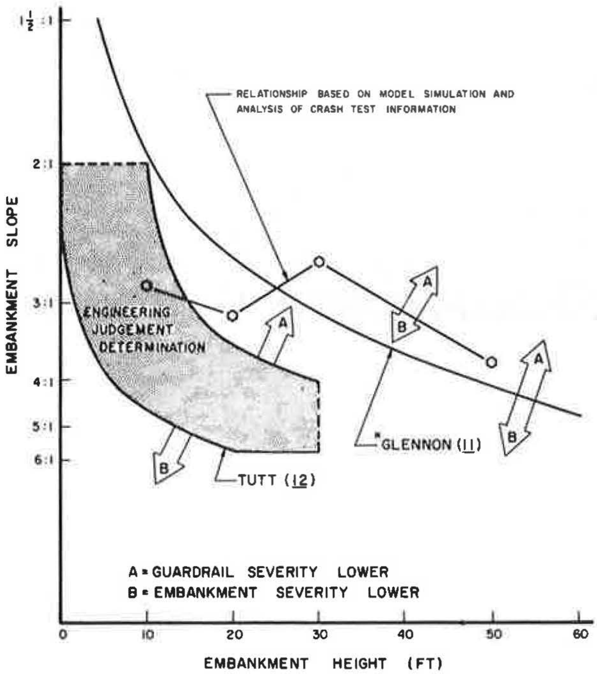

ysis of accident information compiled on the California highways during the years of 1963 and 1964. Their work is currently used by many highway engineers.

As evident in Figure 4, the relation established by Glennon and Tamburri generally agrees with the relation established in this study. The differences existing between these two independently established curves are attributed to the following: The conditions of encroachment of 60 mph and 25 deg investigated in this study are probably more severe than those conditions occurring in the majority of the accidents statistically analyzed, and the Texas guardrail system is stiffer than that used at the time of the accidents because of a smaller post spacing.

A guide to determine if a guardrail is needed on roadway embankments was also presented by Tutt (12) and is shown in Figure 4. As in the criteria presented by Tutt, engineering judgment must be used in applying the results of this study. Where a hazardous condition exists along or at the bottom of the embankment, a guardrail may be warranted in the immediate vicinity of the hazard. It is also noted that the safer option (guardrail versus no guardrail) determined by use of this criterion will not necessarily ensure a safe situation; i.e., severe injuries may still occur. This approach will, however, provide an objective means of selecting the safer of two hazardous situations.

PARAMETER STUDY OF ENCROACHMENT CONDITIONS

In previous sections, severity values for automobiles traversing different embankment heights and slopes and automobiles colliding with guardrails were presented. The encroachment conditions were a speed of 60 mph and an angle of 25 deg. The effects of the encroachment conditions on the vehicle's behavior and the severity of the event were determined by making a series of runs where the speed and encroachment angle were varied. An embankment having a 3:1 slope and a 20-ft height was selected for the study.

The majority of full-scale crash tests on a guardrail have been conducted at an impact speed of 60 mph and an angle of 25 deg. Prediction of the severity of guardrail damage for different conditions of impact was made by using the mathematical equations developed by Olson (9). It was shown earlier that these equations, Eqs. 1 and 2, compare favorably with measured accelerometer information.

Before Eq. 1 could be used, a method was needed to estimate the dynamic displacements D of a guardrail for various conditions of impact. This was done by assuming that the displacement of a guardrail is proportional to the loss in kinetic energy of an automobile as it is being redirected. The kinetic energy KE expended by a guardrail from the instant of impact to the time when the automobile is parallel to the guardrail was approximated as follows:

$$KE = C\left[\frac{1}{2}\frac{W}{g} V_I^2 \sin^2(\theta)\right] \tag{5}$$

Note that $V_I \sin\theta$ is the component of vehicle velocity normal to the guardrail.

Equation 5 does not account for the kinetic energy expended by changes in the vertical and longitudinal velocity components. The C-coefficient is the portion of the kinetic energy of the vehicle expended by the guardrail. The remainder of the energy of impact is expended primarily in sheet metal crushing of the automobile.

Using information from full-scale crash tests, we approximated the dynamic displacement of a guardrail as follows:

$$\left(\frac{D}{KE}\right)_{\text{test}} = \left(\frac{D}{KE}\right)_{\text{selected conditions}}$$

$$\left\{\frac{D}{C\left[\frac{1}{2}\frac{W}{g} V_I^2 \sin^2(\theta)\right]}\right\}_{\text{test}} = \left\{\frac{D}{C\left[\frac{1}{2}\frac{W}{g} V_I^2 \sin^2(\theta)\right]}\right\}_{\text{selected conditions}}$$

Therefore, assuming $C_{test} = C_{selected\ conditions}$

$$(D)_{\substack{selected\\conditions}} = \left[\frac{D}{WV_I^2 \sin^2(\theta)}\right]_{test} \left[WV_I^2 \sin^2(\theta)\right]_{\substack{selected\\conditions}} \tag{6}$$

The values used for the test parameters in Eq. 6 were selected from the tests on the California guardrail system (8- by 8-in. wood posts), as given in Table 3. The test values used were W = 4,570 lb, D = 2.37 ft (average of 4 tests), V_I = 60 mph = 88 ft/sec, θ = 25 deg, and (sin 25 deg) = 0.423. Thus

$$\left[\frac{D}{WV_I^2 \sin^2(\theta)}\right]_{test} = \left[\frac{2.37}{(4,570)(88)^2(0.423)^2}\right] = 3.74 \times 10^{-7}\,\frac{\text{sec}^2}{\text{lb - ft}}$$

Equation 6 was thus reduced to

$$(D)_{\substack{selected\\conditions}} = (3.74 \times 10^{-7})(W\,V_I^2 \sin^2\theta)_{\substack{selected\\conditions}} \tag{7}$$

The properties of the automobile simulated in HVOSM (1963 Ford Galaxie), which are needed in Eqs. 1 through 4 and Eq. 7, were as follows: W = 4,750 lb, AL = 81.52 in., B = 39.50 in., and μ = 0.3. Substitution of the preceding value of W into Eq. 7 gives

$$(D)_{\substack{selected\\conditions}} = (1.78 \times 10^{-3})(V_I^2 \sin^2\theta)_{\substack{selected\\conditions}} \tag{8}$$

In Table 5, values for V_I and θ were inserted in Eq. 8 to compute the guardrail dynamic displacements.

The duration ΔT of the guardrail impact was estimated by using Eq. 9.

$$\Delta T = \frac{V_I \sin\theta}{g\,G^{*}_{lat}} \tag{9}$$

The numerator and denominator of the right-hand side of Eq. 9 are respectively the component of vehicle velocity normal to the guardrail and vehicle acceleration normal to the guardrail.

The computed decelerations and SI's for an automobile redirected by a guardrail for various encroachment conditions are given in Table 5. The tolerable accelerations used to compute the SI's were for the 225- to 450-msec duration (Table B1, 2).

Table 6 gives the results of the parameter study on the selected embankment (3:1 side slope, 20 ft in height). The dynamic behavior of an automobile at speeds of 50, 60, and 70 mph and encroachment angles of 10, 17.5, and 25 deg were investigated by using HVOSM.

SI curves for guardrail and the typical embankment as a function of encroachment conditions are shown in Figure 5. The severity curve for the 25-deg encroachment angle shows a sharp decrease as the speed of the automobile increases from 60 to 70 mph. Intuitively, this phenomenon appears incorrect. However, as discussed in a previous section, at 60 mph the front and rear bumpers of the automobile contacted the ditch bottom simultaneously, causing high resistive forces and accelerations. At 70 mph, front and rear bumper contact did not occur simultaneously, and the resistive forces were lower. For comparative purposes, the SI for a 3.25:1 slope and encroachment conditions of 60 mph and 25 deg (run 7, Table 1) is shown in Figure 5.

It can be seen in Figure 5 that, for a 17.5-deg angle of encroachment or less, embankment severity is less than guardrail severity at all speeds. This suggests that the criteria shown in Figure 3 may require more guardrail than needed for most accident situations because the encroachment angle of most errant vehicles is less than 25 deg.

Table 5. Computed guardrail severity indexes.

Impact Speed (mph)	Impact Angle (deg)	Guardrail Dynamic Displacement (ft)	G^*_{lat} (Eq. 1)	G^*_{long}, Eq. 2 (μ = 0.3)	Time Duration, Eq. 9 (msec)	G_{long} (Eq. 3)	G_{lat} (Eq. 4)	SI
50	10.0	0.29	1.8	0.5	224	0.8	1.7	0.4
50	17.5	0.86	2.8	0.8	249	1.6	2.4	0.7
50	25.0	1.71	3.5	1.1	276	2.1	2.7	0.8
60	10.0	0.41	2.4	0.7	202	1.1	2.2	0.6
60	17.5	1.25	3.5	1.0	237	2.0	3.0	0.8
60	25.0	2.47	4.3	1.3	271	3.0	3.3	1.0
70	10.0	0.57	2.9	0.9	191	1.4	2.7	0.7
70	17.5	1.70	4.1	1.2	233	2.4	3.6	1.0
70	25.0	3.35	4.9	1.5	273	3.4	3.9	1.1

Figure 5. Guardrail and embankment severity as function of encroachment speed and angle.

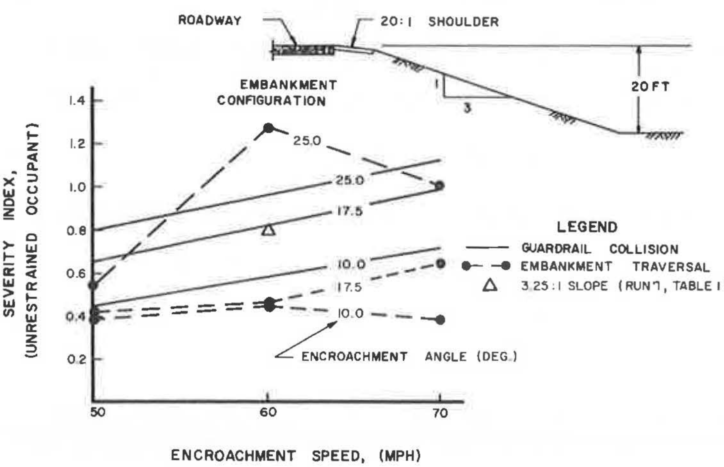

Table 6. Simulation results on 20-ft and 3:1 slope embankment.

Terrain			Automobile									
Run No.	Embankment Height (ft)	Embankment Slope (b:a)	Encroachment Speed (mph)	Encroachment Angle (deg)	Maximum Roll Angle (deg)	Maximum Pitch Angle (deg)	Angle Automobile Contacts Flat Ditch (deg)	Speed Automobile Contacts Flat Ditch (mph)	Average Decelerations >50 msec: G_{long}	G_{lat}	G_{vert}	SI
15	20	3:1	50	10.0	22	8	26	55	0.6	0.5	2.2	0.4
16	20	3:1	50	17.5	25	10	29	55	0.8	0.8	2.2	0.4
17	20	3:1	50	25.0	27	12	35	54	1.3	0.8	2.9	0.5
18	20	3:1	60	10.0	23	7	23	64	0.6	0.5	2.6	0.5
19	20	3:1	60	17.5	27	9	26	64	0.9	1.0	2.4	0.5
5	20	3:1	60	25.0	30	12	40	62	1.3	0.8	7.6	1.3
20	20	3:1	70	10.0	25	6	19	74	0.5	0.6	2.2	0.4
21	20	3:1	70	17.5	31	9	26	73	1.2	1.1	3.5	0.7
22	20	3:1	70	25.0	32	16	37	69	0.1	1.5	6.1	1.1

Note: Shoulder width = 10 ft and shoulder slope = 20:1.

CONCLUSIONS

The paper supports the following conclusions:

1. Criteria are presented for making objective decisions on the need for guardrail protection for embankments. The guardrail system for which these criteria are applicable is the steel W-beam supported on a post spaced at 6-ft, 3-in. centers. The criteria show that, for side slopes flatter than 3:1 and fill heights 40 ft or less, guardrail protection is not warranted.
2. The criteria referred to in conclusion 1 were based on an automobile encroachment condition of 25-deg departure angle and 60-mph speed. The effects of vehicle encroachment speed and angle on the severity of both guardrail impacts and embankment traversals were studied. It was concluded that, for speeds of 50, 60, and 70 mph and for shallow encroachment angles (less than 17.5 deg), a collision with the guardrail (as described in conclusion 1) is higher in severity than traversing a 3:1 embankment with a 20-ft fill height. However, as the speed and angle of departure increase, the severity of traversing the embankment approaches that of striking the guardrail.
3. The analysis techniques used in this study, consisting of both mathematical models and full-scale tests, could be used to develop need criteria for various types of guardrail and for various encroachment conditions.

ACKNOWLEDGMENT

This research was sponsored by the Texas Highway Department in cooperation with the U.S. Department of Transportation, Federal Highway Administration. The contents of this paper reflect the views of the authors who are responsible for the facts and the accuracy of the data presented herein. The contents do not necessarily reflect the official views or policies of the Federal Highway Administration. This paper does not constitute a standard, specification, or regulation.

REFERENCES

1. McHenry, R. R., and Segal, D. J. Determination of Physical Criteria for Roadside Energy Conversion Systems. Cornell Aeronautical Laboratory, Rept. VJ-2251-V-1, July 1967.
2. Ross, H. E., Jr., and Post, E. R. Criteria for Guardrail Need and Location on Embankments—Volume I, Development of Criteria. Texas Transportation Institute, Texas A&M Univ., Res. Rept. 140-4, April 1972.
3. Young, R. D., Edwards, T. C., Bridwell, R. J., and Ross, H. E. Documentation of Input for Single Vehicle Accident Computer Program. Texas Transportation Institute, Texas A&M Univ., Res. Rept. 140-1, July 1969.
4. Hyde, A. S. Biodynamics and the Crashworthiness of Vehicle Structures. Wyle Laboratories, Huntsville, Rept. WR 68-3, March 1968.
5. Weaver, G. D. The Relation of Side Slope Design to Highway Safety. Texas Transportation Institute, Texas A&M Univ., Rept. 626-1, Feb. 1970, p. 29.
6. Tamanini, F. J., and Viner, M. Energy Absorbing Roadside Crash Barriers. ASCE New York, Jan. 1970.
7. Nordlin, E. F., Woodstrom, J. H., and Hackett, R. P. Dynamic Tests of the California Type 20 Bridge Barrier Rail Series XXIII. Materials and Research Laboratory, California Division of Highways, M&R Rept. 636459, Sept. 1970, pp. A6-7.
8. Michie, J. D., Calcote, L. R., and Bronstad, M. E. Guardrail Performance and Design. NCHRP Rept. 129, Jan. 1970.
9. Olson, R. M., Post, E. R., and McFarland, W. F. Tentative Service Requirements for Bridge Rail Systems. NCHRP Rept. 86, 1970, pp. 11-12.
10. Beaton, J. L., Nordlin, E. F., and Field, R. N. Dynamic Tests of Corrugated Metal Beam Guardrail. Highway Research Record 174, 1967, pp. 42-87.
11. Glennon, J. C., and Tamburri, T. N. Objective Criteria for Guardrail Installation. Highway Research Record 174, 1967, pp. 184-206.
12. Tutt, P. R., and Nixon, J. F. Roadside Design Guidelines. HRB Spec. Rept. 107, 1970, p. 124.

13. Young, R. D. A Three-Dimensional Mathematical Model of an Automobile Passenger. Texas Transportation Institute, Texas A&M Univ., Res. Rept. 140-2, Aug. 1970.
14. Highway Research Board Circular 482, Sept. 1962.